DOE/NASA/10350-19
NASA TM-81612

Effect of Fuel Nitrogen and Hydrogen Content on Emissions in Hydrocarbon Combustion

David A. Bittker and Gary Wolfbrandt
National Aeronautics and Space Administration
Lewis Research Center

Work performed for
U.S. DEPARTMENT OF ENERGY
Fossil Energy
Office of Coal Utilization

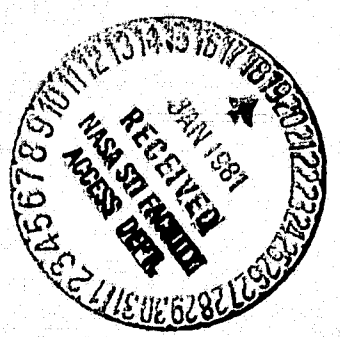

Prepared for
Twenty-six Annual International Gas Turbine Conference
sponsored by American Society of Mechanical Engineers
Houston, Texas, March 8-12, 1981

DOE/NASA/10350-19
NASA TM-81612

Effect of Fuel Nitrogen and Hydrogen Content on Emissions in Hydrocarbon Combustion

David A. Bittker and Gary Wolfbrandt
National Aeronautics and Space Administration
Lewis Research Center
Cleveland, Ohio 44135

Work performed for
U.S. DEPARTMENT OF ENERGY
Fossil Energy
Office of Coal Utilization
Washington, D.C. 20545
Under Interagency Agreement DE-AI01-77ET10350

Prepared for
Twenty-six Annual International Gas Turbine Conference
sponsored by American Society of Mechanical Engineers
Houston, Texas, March 8-12, 1981

EFFECT OF FUEL NITROGEN AND HYDROGEN CONTENT ON EMISSIONS IN HYDROCARBON COMBUSTION

by David A. Bittker and Gary Wolfbrandt

National Aeronautics and Space Administration
Lewis Research Center
Cleveland, Ohio 44135

E-614

INTRODUCTION

This paper presents the results of a study of the effects of operating conditions and fuel properties on emissions during the two-stage combustion of hydrocarbon fuels. This work is part of a theoretical and experimental basic research effort in support of a major Department of Energy program to adapt ground-power gas turbines to use coal derived liquid fuels (1).[1] The importance of this syncrude-burning capability to the development of the gas turbine for ground power is discussed at length in reference (1). One of the important questions is how the emissions of nitrogen oxides (NO_x) and carbon monoxide (CO) will be affected by (1) the increased content of low percentage hydrogen aromatic hydrocarbons and (2) the increased content of organic nitrogen compounds in these coal-derived fuels.

The present work is part of the Critical Research and Technology (CRT) project funded by the Department of Energy at the Lewis Research Center (DOE/NASA Interagency Agreement No. DEAI-01-77ET10350). Its main purpose is to determine, theoretically and experimentally, the effect of operating conditions on nitrogen oxides emissions during syncrude combustion. Under normal combustion conditions most of the chemically bound nitrogen in hydrocarbon fuels will be converted to nitrogen oxides (NO_x) (2 and 3). Two-stage combustion has been suggested by several investigators (4, 5 and 6) as a technique for reducing NO_x emissions. The control of NO_x is achieved by rich primary burning followed by very lean secondary combustion. Lack of oxygen in the rich primary zone reduces the formation of NO_x while the fuel-bound nitrogen (FBN) forms molecular nitrogen and other compounds. In the very lean secondary zone thermal NO_x formation from N_2 is limited by the reduced temperature, while the other nitrogen compounds present react less rapidly to form NO_x than the original FBN. Therefore, a two-stage combustor model was used in a parametric study to extend current knowledge by determining the relationship between operating conditions, fuel properties and exhaust emissions. Although NO_x emissions are the main focus of this work, effects of variables on CO emissions were also investigated.

The preliminary analytical part of this study was reported in reference (7) and the experimental part of the work was reported in reference (8). The present paper reports additional theoretical computations and gives comparisons of theoretical and experimental results for a variety of conditions. The operating conditions used in this work include a primary equivalence ratio, ϕ_p, range of 0.6 to 1.8 and one secondary equivalence ratio, ϕ_s, of 0.5. The primary zone residence time ranged from 12 to 20 msec and secondary residence times from 1 to 3 msec. Fuel-bound nitrogen contents of 0.5 and 1.0 percent were used and fuel hydrogen varied from 9 to 18 weight percent. Initial temperature and pressure were not primary variables in this work. Pressure was generally maintained at 5 atm. However, a limited number of computations was performed at a pressure of 12 atm. Initial temperatures ranged from 600 to 650 K, depending upon composition.

ANALYTICAL COMBUSTOR MODEL AND EXPERIMENTAL DETAILS

Two-stage combustion was studied experimentally in a flame tube with secondary air injection. A diagram of the apparatus is given in figure 1. Fuel

[1] Numbers in parentheses designate references at end of paper.

mixtures of propane, toluene and pyridine were blended to give a range of carbon-hydrogen ratios and fuel nitrogen contents matching syncrude fuel properties. Exhaust gases were sampled for emissions of nitrogen oxides, carbon monoxide, carbon dioxide and unburned hydrocarbons. From these data combustion efficiencies and percent conversion of FBN to NO_x were computed. Complete details of the experimental apparatus and procedure are given in reference (8).

The two-stage flame tube was modeled theoretically by a two-stage, adiabatic well-stirred reactor. A description of the mathematical technique is given in reference (7). This highly back-mixed, idealized system was assumed to approximate the turbulent mixing in the flame tube. The fuels used were propane, tolulene and one mixture of these two fuels. The exhaust gases from the primary-stage reactor were assumed to be instantaneously diluted with the required amount of air and then enter the second-stage reactor. This assumption is one of the major differences between the theoretical model and the experimental flame tube. In the latter there are mixing inhomogeneities caused by the dilution and mixing zone between the end of the primary combustion zone the start of secondary combustion. A second difference between the idealized model and the experimental flame tube is the heat transfer losses for the experiment, which are not considered in the analytical model.

A third difference between the theoretical model and the experiment is the method of adding chemically bound nitrogen to the fuel. In the experiment the organic compound pyridine was blended with the hydrocarbon fuels. For the computations, FBN was added in the form of free nitrogen atoms. The rationale for using this simple "model compound" to represent organic fuel bound nitrogen is described in reference (7). Another difference between the experiment and the computational model is the fact that the chemical model does not take into account smoke formation. In the experimental study (8) a few smoke measurements were made. The results showed relatively high smoking tendencies even at the relatively low pressures used, and with high dilution in the secondary zone. Reference (7) showed that, in spite of these differences between experiment and analytical model, certain experimental trends for propane-air mixtures could be theoretically predicted. In reference (7), comparisons were done only for some preliminary experimental data. In this report a more extensive comparison is given between computed results and experimental data.

CHEMICAL MODEL

The chemistry of nitrogen oxide formation during hydrocarbon combustion has been studied extensively (9 and 10). For the computations of reference (7), a fifty-seven reaction mechanism was used for the propane-air combustion system. The important nitric oxide forming reactions are, first of all, the extended Zeldovich mechanism:

$$N + O_2 \rightleftharpoons NO + O$$

$$O + N_2 \rightleftharpoons NO + N$$

$$N + OH \rightleftharpoons NO + H$$

For rich mixtures, the direct reaction of hydrocarbon fragments with molecular nitrogen:

$$CH + N_2 \rightleftharpoons HCN + N$$

has been found to be important (10 and 11). This reaction is followed by radical attack on HCN and further reactions involving the oxidation of CN, NCO and NH species to NO. For the computations to be reported in this paper several reactions have been added to the mechanism. First of all, two reactions involving hydrocarbon fragments and NO have been added:

$$CH + NO \rightleftharpoons HCN + O$$

$$CH + NO \rightleftharpoons HCO + N$$

These reactions are important for rich primary mixtures. In addition the following three radical attacks on HO_2 radical have been added:

$$O + HO_2 \rightleftharpoons OH + O_2$$

$$H + HO_2 \rightleftharpoons OH + OH$$

$$OH + HO_2 \rightleftharpoons H_2O + O_2$$

These reactions are important mainly for lean and stoichiometric primary mixtures. The nitrogen oxides are mostly nitric oxide, NO, especially for rich primary mixtures. For lean and stoichiometric mixtures some NO is converted to nitrogen dioxide, NO_2, by the reactions

$$HO_2 + NO \rightleftharpoons OH + NO_2$$

$$O + NO_2 \rightleftharpoons NO + O_2$$

Total NO_x was always taken as the sum of the NO and NO_2 concentrations. The complete mechanism used for propane-air combustion and NO_x formation is given in table I. When tolulene is included in the fuel, additional reactions are needed in the oxidation mechanism. The recent work of McLain, Jachimowski and Wilson (12) has provided the first detailed oxidation mechanism for toluene. The additional reactions used in the present computation, when toluene is in the fuel mixture, are given in table II.

RESULTS AND DISCUSSION

Effect of Fuel-Bound Nitrogen on NO_x Formation

The results of this study are presented for three different fuels, A, B and C. Fuel A contains nominally 18 percent hydrogen by weight, fuel B is 11 percent and fuel C contains 9 percent hydrogen. Fuel A is pure propane both for the computations and the experimental work. Fuel B is, for the computations, a mixture of 26.74 percent propane and 73.26 percent toluene by weight. Nitrogen atoms are added to give the appropriate amount of fuel bound nitrogen. Experimentally, fuel B is either the stated mixture of propane and toluene (for zero percent FBN) or the appropriate mixture of propane, toluene and pyridine when FBN is present. Fuel C is, computationally, pure toluene with nitrogen atoms added for FBN. Experimentally, fuel C is a mixture of either toluene and propane or toluene, pyridine and propane.

Figure 2(a) shows computed final (second-stage) NO_x concentration as a function of primary equivalence ratio, ϕ_p, for fuel A with 0, 0.5 and 1.0 percent fuel-bound nitrogen (FBN) contents. These

results are slightly different from those presented in reference (7) because of the expanded chemical model used here. However, the same trends are shown. Minimum NO_x formation occurs for a ϕ_p value of about 1.5. Although NO_x emission increases with FBN content, the conversion of FBN to NO_x decreases as the amount of FBN increases. This is shown by the curves' getting closer together as FBN content increases. Computed NO_x emissions for fuel B are shown in figure 2(b). The general trends with ϕ_p and FBN content are similar to those for fuel A. Although results could not be obtained for rich ϕ_p values above 1.5, the ϕ_p values for minimum NO_x formation are definitely greater than 1.5 for all three nitrogen contents. For fuel C, the lowest hydrogen content fuel, computed NO_x concentration vs ϕ_p results were obtained up to $\phi_p = 1.6$. The plots in figure 2(c) show trends with ϕ_p and FBN content similar to the other fuels. However, it appears that the ϕ_p value for minimum NO_x emission is now greater than 1.6. Thus the computed results indicate an increase in the ϕ_p for minimum NO_x with decreasing hydrogen content of the fuel. This trend agrees with the experimental results previously published (8). A full comparison of computed and experimental NO_x emission concentrations will be given in the next section.

A detailed study of the computed results indicates a possible explanation for the shift of the ϕ_p value for minimum NO_x as the amount of aromatic hydrocarbon in the fuel increases. The pyrolysis reactions of toluene (see table II) form significant amounts of hydrocarbon fragments that are not present during the pyrolysis and oxidation of propane. The reactions of these fragments form CH radicals which destroy NO directly via reactions 58 and 59 of table I. We have determined that the importance of these reactions increases significantly as the percentage of toluene in the fuel increases. This additional path for NO reaction increases the ratio between its destruction and its formation by reactions such as the oxidation of nitrogen atoms and HCN species by hydroxyl radical, OH. Therefore, as more toluene is added to the fuel, the minimum NO_x concentration occurs at increasingly higher ϕ_p values.

We have shown directly the effect of ϕ_p on percent FBN conversion to NO_x in figure 3, which gives this percent conversion plotted against ϕ_p for all three fuels. Computed results for fuel A are shown in figure 3(a). FBN conversion is lower for the 1.0 percent fuel nitrogen content than for the 0.5 percent content. Moreover, the conversion is smallest in the rich ϕ_p region of 1.4 to 1.5 where NO_x emissions are at their minimum. No flame tube experiments with added fuel nitrogen were performed for fuel A, so only computed results are shown. In figure 3(b) it is seen that, for fuel B, the computed difference in fuel nitrogen conversion between 0.5 and 1.0 percent FBN contents is quite small, even though the 1.0 percent FBN values are still lower. Experimental flame tube data are also plotted. The two points that can be compared with the computed lines are in excellent agreement with them. All the experimental data are consistent with the computed trend of slightly lower FBN conversion for the higher FBN content fuel. A much better comparison of experimental and computed conversions is shown in figure 3(c) for fuel C. The computed results for ϕ_p values ≤ 1.1 indicate the conversion to NO_x is significantly lower for 1.0 percent FBN content then for 0.5 percent FBN. However for ϕ_p values greater than 1.1, the percents conversion are very close for the two FBN contents. The experimental data points shown are in good qualitative agreement with these computed trends and also in good quantitative agreement with the computed results for rich primary equivalence ratios. It is significant to note that FBN conversion rates of less than 10 percent can be achieved with rich-lean, two-stage combustion.

Effect of Hydrogen Content on NO_x Formation

The computed effect of hydrogen content on NO_x emissions is shown in figure 4. The final NO_x concentration, plotted against primary equivalence ratio for the three fuels used, is shown in figure 4(a) for no fuel bound nitrogen content. For ϕ_p values up to about 1.5, NO_x concentration increases as the fuel hydrogen content decreases. However, at $\phi = 1.6$, the computed NO_x concentration is the same for the 9 percent and the 18 percent hydrogen fuels. Similar situations can be seen in figures 4(b) and (c) which show the same type of plot for the three fuels with 0.5 and 1.0 percent FBN content. In these plots two trends are noticeable. First, the effect of decreasing the hydrogen content becomes smaller as the hydrogen percentage decreases. Second, the presence of fuel nitrogen appears to lessen the NO_x increase caused by lowering the fuel hydrogen content. Therefore, the computations predict that hydrogen content has a small effect on NO_x emission at rich equivalence ratios in this two-stage combustion. The experimental results agree with this predicted trend, as can be seen by examining the experimental data also plotted in figures 4(a) to (c). For rich primary mixtures these data indicate essentially the same NO_x emissions for fuels B and C, whose hydrogen contents are 11 and 9 percent. Quantitatively, the theoretical model predicts too little NO_x for rich primary mixtures and over predicts NO_x for lean primary mixtures. The lean side effect is mainly due to lack of heat-loss corrections in the model. This results in higher computed reaction temperatures and thus too much thermal NO_x formation. For the rich primary mixtures deficiencies in the gas-phase chemical mechanism for the conversion of fuel nitrogen to NO_x may explain a good part of the discrepancies. In figure 4(c) we have also shown experimental data (the filled-in diamond symbols) for NO_x emissions using an actual coal syncrude fuel. The fuel was made by the SRC-II process and is a 2.9:1 blend of middle and heavy distillates. The hydrogen content is 8.64 weight percent and the bound nitrogen content is 0.95 percent. Detailed properties of this fuel are given in table I of reference (8). It can be seen that there is good agreement between measured NO_x for the actual syncrude fuel and for the toluene-propane-pyridine simulated syncrude fuel.

Effect of Fuel Nitrogen and Hydrogen Content on CO Emission

The effect of both hydrogen and nitrogen content of the fuel on CO emission is shown in figure 5. Final CO concentration is plotted against ϕ_p for the three different fuels. In figure 5(a) the fuels contain no nitrogen. In figures 5(b) and (c) the fuels contain 0.5 and 1.0 percent FBN. For all nitrogen contents we see that the computed CO concentration increases significantly as hydrogen content of the fuel decreases. By comparing curves for the same fuel in figures 5(a) to (c) it can readily be seen that computed CO concentration is independ-

ent of fuel-bound nitrogen content. Theoretically, it would be expected that CO formation would increase with decreasing hydrogen to carbon ratio of a hydrocarbon fuel from equilibrium thermodynamic considerations, without any chemical kinetics. Therefore, the observed increase in CO emissions with decreasing hydrogen content of our three fuels is not surprising. Experimental verification of this trend for two-stage combustion can be seen in figure 5(a). The data points plotted show considerable scatter. However, they follow the trend of the computed curves with ϕ_p. For this condition of no added fuel bound nitrogen, the data indicate a generally increasing CO level as hydrogen content decreases. The experimental data in figures 5(b) and (c) are insufficient to determine any CO trend with hydrogen content. However, they follow the computed trend with ϕ_p and also verify the lack of dependence of CO concentration on fuel bound nitrogen content found theoretically.

Effect of Residence Times on NO_x and CO Emissions

Previous theoretical computations (7) for fuel A showed that NO_x and CO emissions are independent of primary-stage residence time. The experimental results (8) showed an increase of NO_x concentration with increasing primary-zone residence time for fuel C. These experimental results are shown in figure 6 along with theoretical computations for fuel C. The data shown are for a primary equivalence ratio of 1.6. The computations show the same NO_x independence of primary-zone volume (i.e., residence time) as found for fuel A. The experimental results show an increase of about 16 percent in NO_x formation when the primary-zone residence time increases by about 19 percent. The failure of the model to predict this trend is no doubt due to its lack of heat-loss corrections and inability to simulate the finite experimental mixing of air with the primary combustion gases.

The theoretical computations (7) for fuel A indicated some increase of NO_x formation with increasing secondary residence time. This was true only for rich primary mixtures, diluted to a secondary equivalence ratio of 0.7. When these rich mixtures were diluted to $\phi_s = 0.5$, the NO_x formation was found to be constant as secondary residence time increased. In figures 7(a) and (b) we have plotted NO_x concentration vs. secondary residence time for fuels B and C to see the effect of fuel hydrogen content. Only $\phi_s = 0.5$ was used for the computations. It is apparent that NO_x concentration is generally independent of secondary residence time for these lower hydrogen-content fuels. Very slight increases can be seen for the richest ϕ_p values of 1.4 and 1.6. Experimental results for fuel B are shown in figure 8, where NO_x concentration is plotted against secondary equivalence ratio for several secondary residence times and $\phi_p = 1.5$. These data shown a very slight effect of secondary residence times at $\phi_s = 0.5$ and a significant increase in NO_x with secondary residence time for $\phi_s = 0.6$ and 0.7. These experimental results are in agreement with the computed trends. We have found that fuel hydrogen content has no effect on the NO_x trend with secondary residence time.

Figures 9(a) and (b) show plots of computed CO concentration against secondary residence time for fuels B and C. Fuel nitrogen content is 0.5 percent, as in figure 7. The trends are the same as found for fuel A in reference (7). The CO emission decreases significantly with increasing residence time. Thus, one can decrease the CO emission without increasing NO_x by increasing the secondary residence time. This is particularly important because of the increased level of CO emissions in these lower hydrogen content fuels.

Effect of Pressure on NO_x Formation

Although pressure was not a primary variable in this study, a limited number of computations was performed at a higher pressure of 12 atm. Fuel B was used. Computations were performed for fuel nitrogen contents of 0 and 0.5 percent over a ϕ_p range of 0.8 to 1.5. Plots of final NO_x and CO concentration vs. ϕ_p for pressures of 5 and 12 atm are shown in figures 10 and 11 for the two nitrogen contents. Results show that increasing the pressure causes a small to moderate increase in NO_x concentration at most ϕ_p values. For the rich ϕ_p values of most interest the increase is 30 percent for no FBN and only 3 percent for 0.5 percent FBN. All the NO_x increase is due to the thermal NO_x. The computed percents conversion of fuel nitrogen to NO_x are slightly lower at 12 atmospheres pressure than at 5 atm. Carbon monoxide formation decreases at the higher pressure. It was not possible to perform experiments at high pressure to obtain data to compare with the computed results.

SUMMARY OF RESULTS

An experimental and theoretical study has been made of the effect of operating conditions and fuel properties on emissions during two-stage syncrude combustion. The hydrogen content of the fuel was varied from 18 percent (pure propane) to 9 percent (pure toluene). Nitrogen content of each fuel was changed from zero up to 1.0 percent by weight. Primary-stage equivalence ratio was varied from 0.6 to 1.8 and second-stage dilution was always to an equivalence ratio of 0.5. Pressure was usually held constant at 0.48 MPa (5 atm) and inlet mixture temperatures varied from 600 to 650 K, depending upon its composition. Nitrogen oxides and carbon monoxide emissions were computed using a two-stage, well-stirred reactor combustor model and were measured experimentally using a two-stage, highly turbulent flame tube. The results of this study may be summarized as follows:

1. The simple stirred-reactor model was able to predict several of the important trends for the emissions from two-stage hydrocarbon combustion.

2. Two-stage, rich-lean combustion gives experimental conversion rates of fuel-bound nitrogen to NO_x of 10 percent or less for rich equivalence ratios of 1.5 to 1.7 and fuel-bound nitrogen contents of 0.5 and 1.0 percent by weight. These results of the experimental flame-tube work are the same as those predicted by the two-stage well-stirred reactor computations.

3. Both experiment and theory show that decreasing fuel hydrogen content causes a small increase in NO_x emission level. The presence of fuel nitrogen may decrease the effect of hydrogen content on NO_x.

4. Although the absolute level of NO_x emission increases with fuel-bound nitrogen content, the percent conversion of the fuel nitrogen decreases slightly as the amount of fuel nitrogen increases. This is found both experimentally and theoretically.

5. Both experimentally and theoretically, the rich primary equivalence ratio for minimum NO_x formation shifts to higher values as the amount of aromatic hydrocarbon (toluene) in the fuel is increased. This can be explained by the reaction of

the pyrolysis products of toluene directly with NO to increase the NO destruction rate.

6. Carbon monoxide emissions increase significantly with decreasing fuel hydrogen content, as shown by both the experiments and the theoretical computations. Also CO emissions are highest at the rich primary equivalence ratios that give minimum NO_x.

7. Both experiments and theoretical computations show that carbon monoxide emissions are independent of fuel-bound nitrogen content.

8. The formation of NO_x increases slightly at most primary equivalence ratios when the pressure is increased from 5 to 12 atm. The increase is between 3 and 30 percent at the rich equivalence ratios for minimum NO_x formation. All the increase is due to thermal NO_x. The percent conversion of fuel-bound nitrogen at 12 atm is slightly less than at 5 atm.

9. Computed NO_x emissions are essentially indendent of secondary residence time for all fuels used, when the secondary equivalence ratio is 0.5.

10. Computed CO emission decreases significantly as secondary residence time increases for all fuels used and all operating conditions.

11. Computed NO_x and CO emissions are independent of primary-zone residence time. Experimental NO_x emissions, however, increase moderately with primary residence time.

CONCLUDING REMARKS

Although the theoretical and experimental combustors used in this study are not actual gas turbine combustors, the results obtained have some application to more practical combustors. Experimentally, a coal syncrude distillate of the SRC-II process gave NO_x emissions that matched very well those from the fuel blends used to simulate the actual fuels in both hydrogen and nitrogen content. Limited measurements of smoke from the rich-lean combustion of these simulated syncrude fuels indicated relatively high smoke emissions in spite of the very lean second-stage burning. This fact, along with the high observed carbon monoxide emissions, indicates that trade-offs will be necessary between the conditions that minimize NO_x and those that control CO and smoke emissions.

REFERENCES

1. Lister, E., Niedzwiecki, R. W., and Nichols, L., "Low NO_x Heavy Fuel Combustor Program," ASME Paper 80-GT-69, Mar. 1980.

2. Pillsbury, P. W., et al., "Fuel Effects in Recent Combustion Turbine Burner Tests of Six Coal Liquids," ASME Paper 79-GT-137, Mar. 1979.

3. Wilkes, C. and Russell, R. C., "The Effects of Fuel Bound Nitrogen Concentration and Water Injection on NO_x Emissions from a 75-MW Gas Turbine," ASME Paper 78-GT-89, Apr. 1978.

4. Yamagishi, K. et al., "A Study of NO_x Emission Characteristics in Two-Stage Combustion," Symposium (International) on Combustion, 15th; Combustion Institute, Pittsburgh, Pa., 1975, pp. 1157-66.

5. Martin, F. J. and Dederick, P. K., "Nitrogen Oxides from Fuel Nitrogen in Two-Stage Combustion," Symposium (International) on Combustion, 16th, Combustion Institute, Pittsburgh, Pa., 1977, pp. 191-198.

6. Gerhold, B. W., Fenimore, C. P., and Dederick, P. K., "Two-Stage Combustion of Plain and N Doped Oil," Symposium (International) on Combustion, 17th, Combustion Institute, Pittsburgh, Pa., 1978, pp. 703-713.

7. Bittker, D. A., "An Analytical Study of Nitrogen Oxides and Carbon Monoxide Emissions in Hydrocarbon Combustion with Added Nitrogen," ASME Paper 80-GT-60, Mar. 1980.

8. Shultz, D. F. and Wolfbrandt, G., "Flame Tube Parametric Studies for Control of Fuel Bound Nitrogen Using Rich-Lean Two-Stage Combustion," DOE/NASA/2593-80/15, NASA TM 81472, Apr. 1980.

9. Haynes, B. S., "Kinetics of Nitric Oxide Formation in Combustion." Alternative Hydrocarbon Fuels: Combustion and Chemical Kinetics, C. T. Bowman and J. Birkeland, eds., AIAA, New York, 1978, pp. 359-394.

10. Bowman, C. T., "Kinetics of Pollutant Formation and Destruction in Combustion," Progress in Energy and Combustion Science, Vol. 1, No. 1, 1975, pp. 33-45.

11. Fenimore, C. P., "Formation of Nitric Oxide in Premixed Hydrocarbon Flames," Symposium (International) on Combustion, 13th, Combustion Institute, Pittsburgh, Pa., 1971, pp. 373-380.

12. McLain, A. G., Jachimowski, C. J., and Wilson, C. H., "Chemical Kinetic Modeling of Benzene and Toluene Oxidation Behind Shock Waves," NASA TP-1472, Aug. 1979.

13. Wakelyn, N. T., Jachimowski, C. J. and Wilson, C. H., "Experimental and Analytical Study of Nitric Oxide Formation During Combustion of Propane in a Jet-Stirred Combustor," NASA TP 1181, 1978.

14. Jachimowski, Casimir J., "An Experimental and Analytical Study of Acetylene and Ethylene Oxidation Behind Shock Waves," Combustion and Flame, Vol. 29, No. 1, 1977, pp. 55-66.

15. Olson, D. B. and Gardiner, W. C., Jr., "Combustion of Methane in Fuel-Rich Mixtures," Combustion and Flame, Vol. 32, No. 2, June 1978, pp. 151-161.

16. Baulch, D. L., et al., Evaluated Kinetic Data for High Temperature Reactions, Vol. 1: Homogeneous Gas-Phase Reactions of the H_2-O_2 System. Butterworth, London, 1972.

17. Baulch, D. L., et al., Evaluated Kinetic Data for High Temperature Reactions, Vol. 3: Homogeneous Gas-Phase Reactions of the O_2-O_3 System, the CO-O_2-H_2 System and of Sulphur-Containing Species, Butterworth, London, 1976.

18. Hampson, R. F., Jr. and Garvin, D., eds., "Reaction Rate and Photochemical Data for Atmospheric Chemistry-1977," NBS-SP-513, National Bureau of Standards, Washington, D.C., May 1978.

19. Monat, J. P., Hanson, R. K., and Kruger, C. H., "Shock Tube Determination of the Rate Coefficient for the Reaction N_2+O NO+N," Symposium (International) on Combustion, 17th, Combustion Institute, Pittsburgh, Pa., 1979, pp. 543-52.

20. Craig, R. A. and Pritchard, H. O., "Analysis of a Proposal for NO Abatement in Jet Aircraft Engines," Canadian Journal of Chemistry, Vol. 55, No. 10, May 15, 1977, pp. 1599-1608.

21. Schaub, W. M., and Bauer, S. H., "The Reduction of Nitric Oxide during Combustion of Hydrocarbons: Methodology for a Rational Mechanism," Combustion and Flame, Vol. 32, No. 1, May 1978, pp. 35-55.

22. Tunder, R., Mayer, S., Cook, E. and Schieler, I., "Compilation of Reaction Rate Data for Nonequilbrium Performance and Reentry Calculation Programs," TR 1001/9210-02/-1, Aerospace Corp., El Segundo, Calif., Jan. 1967.

TABLE I. - REACTIONS FOR PROPANE-AIR COMBUSTION AND NO_x FORMATION

Reaction number	Reaction	Rate constant[a,b]			Reference
		A	n	θ	
1	$M + C_3H_8 \rightleftharpoons C_2H_5 + CH_3 + M$	5.0×10^{15}	0.0	32 713	13
2	$C_2H_5 \rightleftharpoons C_2H_4 + H$	3.16×10^{13}		20 483	
3	$O + C_2H_4 \rightleftharpoons CH_3 + HCO$	2.26×10^{13}		1 359	
4	$O + C_2H_4 \rightleftharpoons CH_2O + CH_2$	2.5×10^{13}		2 516	
5	$CH_3 C_3H_8 \rightleftharpoons CH_4 + C_3H_7$	2.0×10^{13}		5 184	
6	$C_3H_7 \rightleftharpoons C_2H_4 + CH_3$	4.0×10^{13}		16 658	
7	$H + C_2H_4 \rightleftharpoons H_2 + C_2H_3$	1.1×10^{14}		4 278	
8	$OH + C_2H_4 \rightleftharpoons H_2O + C_2H_3$	1.0×10^{14}		1 761	
9	$M + C_2H_3 \rightleftharpoons C_2H_2 + H + M$	3.0×10^{16}		20 382	
10	$O + C_2H_2 \rightleftharpoons CH_2 + CO$	5.2×10^{13}		1 862	14
11	$M + CH_4 \rightleftharpoons CH_3 + H + M$	4.7×10^{17}		46 900	15
12	$H + CH_4 \rightleftharpoons CH_3 + H_2$	1.26×10^{14}		5 989	13
13	$O + CH_4 \rightleftharpoons CH_3 + OH$	2.0×10^{13}		4 640	
14	$OH + CH_4 \rightleftharpoons CH_3 + H_2O$	3.0×10^{13}		3 020	
15	$CH + O_2 \rightleftharpoons HCO + O$	1.0×10^{13}		0.0	
16	$CH_2 + O_2 \rightleftharpoons CH_2O + O$	1.0×10^{14}		1 862	15
17	$CH_3 + O_2 \rightleftharpoons CH_2O + OH$	1.7×10^{12}		7 045	13
18	$CH_3 + O \rightleftharpoons CH_2O + H$	6.8×10^{13}		0.0	15
19	$CH_2O + H \rightleftharpoons HCO + H_2$	2.0×10^{13}		1 660	
20	$CH_2O + O \rightleftharpoons HCO + OH$	5.0×10^{13}		2 300	
21	$CH_2O + OH \rightleftharpoons HCO + H_2O$	5.0×10^{15}		6 540	
22	$HCO + O \rightleftharpoons CO + OH$	3.0×10^{13}		0.0	
23	$HCO + H \rightleftharpoons CO + H_2$	2.0×10^{13}		0.0	
24	$HCO + OH \rightleftharpoons CO + H_2O$	3.0×10^{13}		0.0	
25	$M + HCO \rightleftharpoons H + CO + M$	3.0×10^{14}		7 397	
26	$CO + OH \rightleftharpoons CO_2 + H$	4.0×10^{12}		4 026	
27	$M + CO + O \rightleftharpoons CO_2 + M$	2.8×10^{13}		-2 285	
28	$CO + O_2 \rightleftharpoons CO_2 + O$	1.2×10^{11}		17 615	
29	$H + O_2 \rightleftharpoons OH + O$	2.2×10^{14}		8 450	16
30	$O + H_2 \rightleftharpoons OH + H$	1.8×10^{10}	1.0	4 480	16
31	$H_2 + OH \rightleftharpoons H_2O + H$	5.2×10^{13}	.0	3 270	15
32	$OH + OH \rightleftharpoons O + H_2O$	6.3×10^{12}		550	16
33	$H + O_2 + M \rightleftharpoons HO_2 + M$	1.5×20^{15}		-503	16
34	$O + O + M \rightleftharpoons O_2 + M$	5.7×10^{13}		-900	17
35	$H + H + M \rightleftharpoons H_2 + M$	8.3×10^{17}	-1.0	0.0	16
36	$H + OH + M \rightleftharpoons H_2O + M$	8.4×10^{21}	-2.0	0.0	16
37	$H + CH_3 \rightleftharpoons H_2 + CH_2$	2.7×10^{11}	.67	12 930	13
38	$O + CH_3 \rightleftharpoons OH + CH_2$	1.9×10^{11}	.68	12 930	13
39	$OH + CH_3 \rightleftharpoons H_2O + CH_2$	2.7×10^{11}	.67	12 930	13
40	$HO_2 + NO \rightleftharpoons NO_2 + OH$	1.2×10^{13}	.0	1 200	18
41	$O + NO_2 \rightleftharpoons NO + O_2$	1.0×10^{13}		300	
42	$NO + O + M \rightleftharpoons NO_2 + M$	5.6×10^{15}		-584	
43	$NO_2 + H \rightleftharpoons NO + OH$	2.9×10^{14}		400	
44	$N + O_2 \rightleftharpoons NO + O$	6.4×10^{9}	1.0	3 145	13
45	$O + N_2 \rightleftharpoons NO + N$	1.8×10^{14}	.0	38 370	19
46	$N + OH \rightleftharpoons NO + H$	4.0×10^{13}		0.0	20
47	$CH + N_2 \rightleftharpoons HCN + N$	1.5×10^{11}		9 562	13
48	$CN + H_2 \rightleftharpoons HCN + H$	6.0×10^{13}		2 669	
49	$O + HCN \rightleftharpoons OH + CN$	1.4×10^{11}	.68	8 506	
50	$OH + HCN \rightleftharpoons H_2O + CN$	2.0×10^{11}	.60	2 516	
51	$CN + O_2 \rightleftharpoons NCO + O$	3.2×10^{13}		503	
52	$CN + CO_2 \rightleftharpoons NCO + CO$	3.7×10^{12}		0.0	
53	$O + NCO \rightleftharpoons NO + CO$	2.0×10^{13}			
54	$N + NCO \rightleftharpoons N_2 + CO$	1.0×10^{13}			
55	$H + NCO \rightleftharpoons NH + CO$	2.0×10^{13}			
56	$NH + OH \rightleftharpoons N + H_2O$	5.0×10^{11}	.5	1 006	
57	$CH + NO \rightleftharpoons N + HCO$	1.0×10^{14}	.0	0.0	21
58	$CH + NO \rightleftharpoons O + HCN$	1.0×10^{13}	.0	0.0	21
59	$CH + CO_2 \rightleftharpoons HCO + CO$	3.7×10^{12}	.0	0.0	13
60	$H + CH_2 \rightleftharpoons H_2 + CH$	2.9×10^{11}	.7	13 080	22
61	$O + CH_2 \rightleftharpoons OH + CH$	3.2×10^{11}	.5	13 080	22
62	$OH + CH_2 \rightleftharpoons H_2O + CH$	5.0×10^{11}	.5	3 019	22
63	$H + HO_2 \rightleftharpoons OH + OH$	2.5×10^{14}	.0	960	15
64	$O + HO_2 \rightleftharpoons OH + O_2$	5.0×10^{13}	.0	503	15
65	$OH + HO_2 \rightleftharpoons H_2O + O_2$	5.0×10^{13}	.0	503	15

[a]Rate constant is given by the equation $k = AT^n \exp(-\theta/T)$, where T is temperature in K and θ is the ratio of the reaction activation energy to the universal gas constant, also in K.

[b]Units of k are sec^{-1} for a unimolecular reaction; for a biomolecular reaction they are $cm^3/mole\text{-}sec$ and for a termolecular reaction $cm^6/mole^2\text{-}sec$.

TABLE II. - REACTIONS FOR TOLUENE OXIDATION

Reaction number	Reaction	Rate constant[a,b]			Reference
		A	n	θ	
66	$C_7H_8 + O_2 \rightleftarrows C_7H_7 + HO_2$	1.0×10^{14}	0.0	20 130	12
67	$C_7H_8 \rightleftarrows C_7H_7 + H$	3.2×10^{15}		44 440	
68	$H + C_7H_8 \rightleftarrows C_7H_7 + H_2$	1.0×10^{14}		3 420	
69	$O + C_7H_8 \rightleftarrows C_7H_7 + OH$	1.0×10^{14}		3 625	
70	$OH + C_7H_8 \rightleftarrows C_7H_7 + H_2O$	1.0×10^{13}		1 510	
71	$O + C_7H_7 \rightleftarrows CH_2O + C_6H_5$	1.0×10^{13}		0.0	
72	$C_7H_7 \rightleftarrows C_4H_3 + C_3H_4$	1.0×10^{15}		51 330	
73	$C_3H_4 \rightleftarrows C_2H_2 + CH_2$	1.0×10^{15}		51 330	
74	$C_3H_4 \rightleftarrows CH_3 + C_2H$	1.0×10^{15}		51 330	
75	$O + C_3H_4 \rightleftarrows C_2H_3 + HCO$	1.0×10^{13}		0.0	
76	$O_2 + C_7H_7 \rightleftarrows 2CO + C_3H_5 + C_2H_2$	5.0×10^{12}		7 550	
77	$C_3H_5 \rightleftarrows CH_3 + C_2H_2$	1.0×10^{14}		27 180	
78	$C_3H_5 \rightleftarrows C_3H_4 + H$	1.3×10^{13}		30 790	
79	$C_2H + O_2 \rightleftarrows HCO + CO$	1.0×10^{13}		3 523	14
80	$C_7H_8 \rightleftarrows C_6H_5 + CH_3$	1.0×10^{17}		52 550	12
81	$C_6H_5 \rightleftarrows C_4H_3 + C_2H_2$	3.2×10^{14}		43 280	
82	$C_4H_3 \rightleftarrows C_2H + C_2H_2$	1.0×10^{14}		29 700	
83	$C_4H_3 \rightleftarrows C_4H_2 + H$	1.0×10^{14}		29 700	
84	$O_2 + C_6H_5 \rightleftarrows 2CO + C_2H_3 + C_2H_2$	7.5×10^{13}		7 550	
85	$H + C_2H_2 \rightleftarrows C_2H + H_2$	2.0×10^{14}		9 562	14
86	$O + C_2H_2 \rightleftarrows C_2H + OH$	3.2×10^{15}	-.6	8 556	
87	$OH + C_2H_2 \rightleftarrows C_2H + H_2O$	6.0×10^{12}	.0	3 523	
88	$O + C_2H \rightleftarrows CO + CH$	5.0×10^{13}		0.0	
89	$O_2 + C_2H_2 \rightleftarrows 2HCO$	4.0×10^{12}		14 090	
90	$M + C_2H_2 \rightleftarrows C_2H + H + M$	1.0×10^{14}		57 370	
91	$O + C_3H_5 \rightleftarrows C_2H_4 + HCO$	1.0×10^{13}		0.0	c

[a]Rate constant is given by the equation $k = AT^n \exp(-\theta/T)$, where T is temperature in K and θ is the ratio of the reaction activation energy to the universal gas constant, also in K.

[b]Units of k are sec^{-1} for a unimolecular reaction; for a biomolecular reaction they are $cm^3/mole\text{-}sec$ and for a termolecular reaction $cm^6/mole^2\text{-}sec$.

[c]Estimate - by analogy with reaction 75.

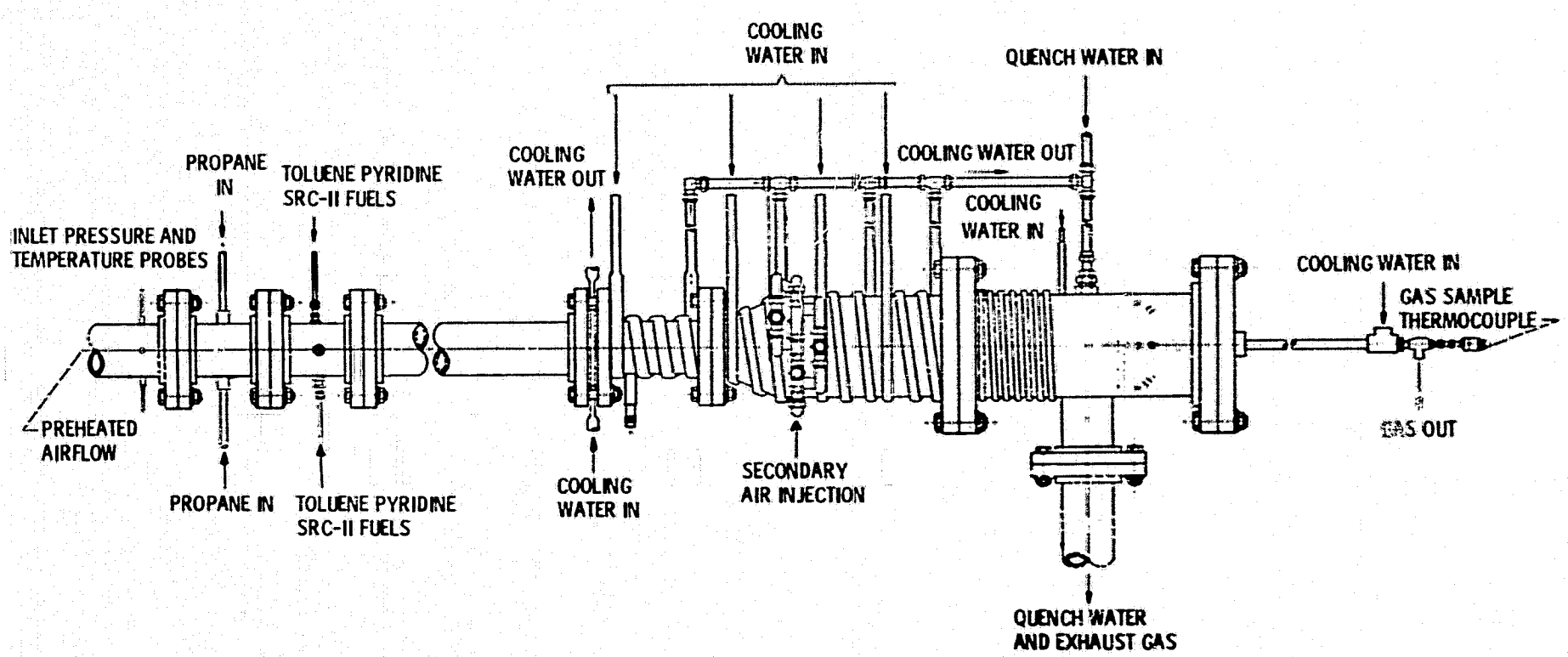

Figure 1. - CRT Flame tube apparatus.

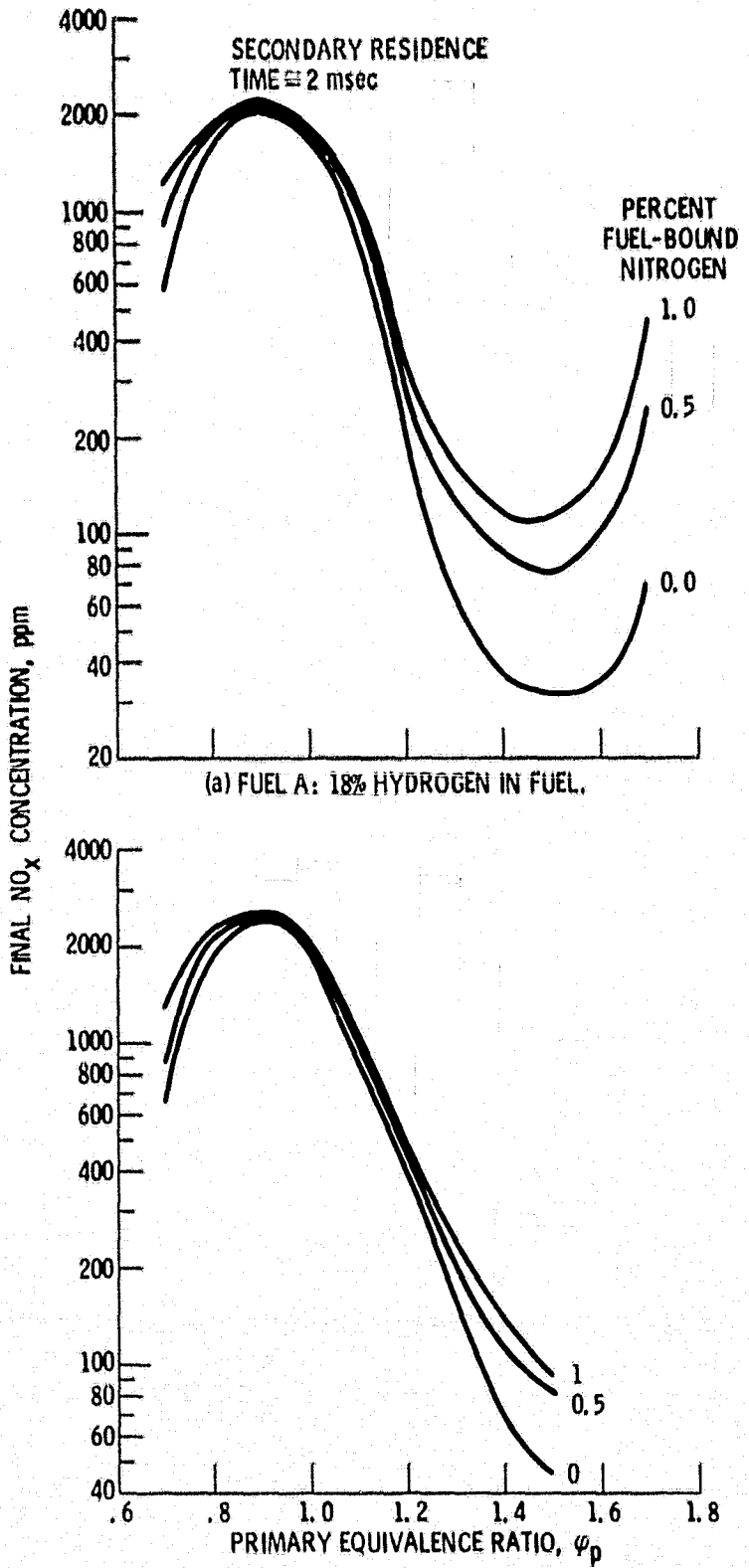

Figure 2. - Computed NO_x concentration vs. primary equivalence ratio. Secondary equivalence ratio = 0.5.

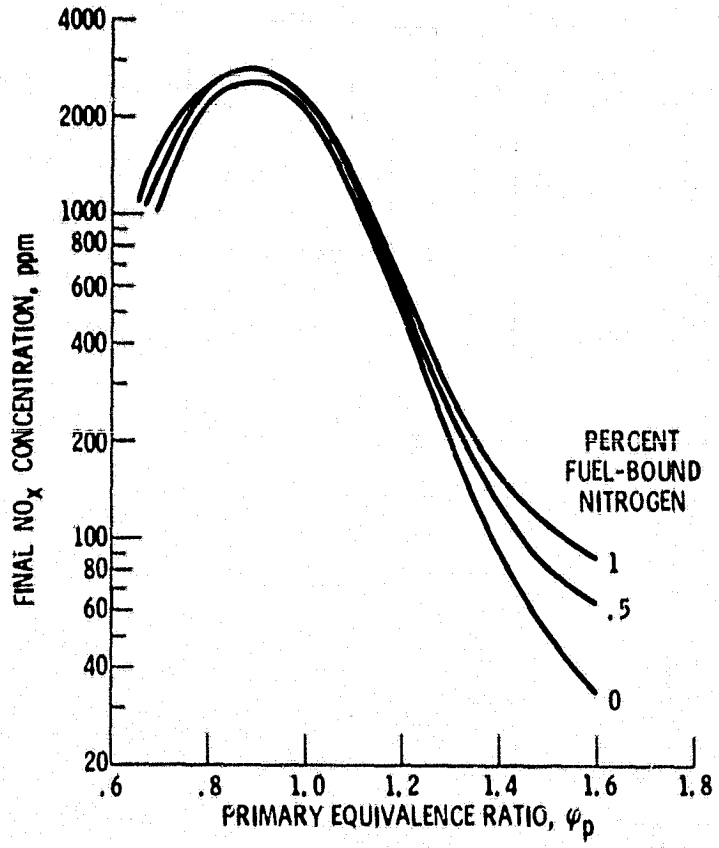

(c) FUEL C: 9 PERCENT HYDROGEN.

Figure 2. - Concluded.

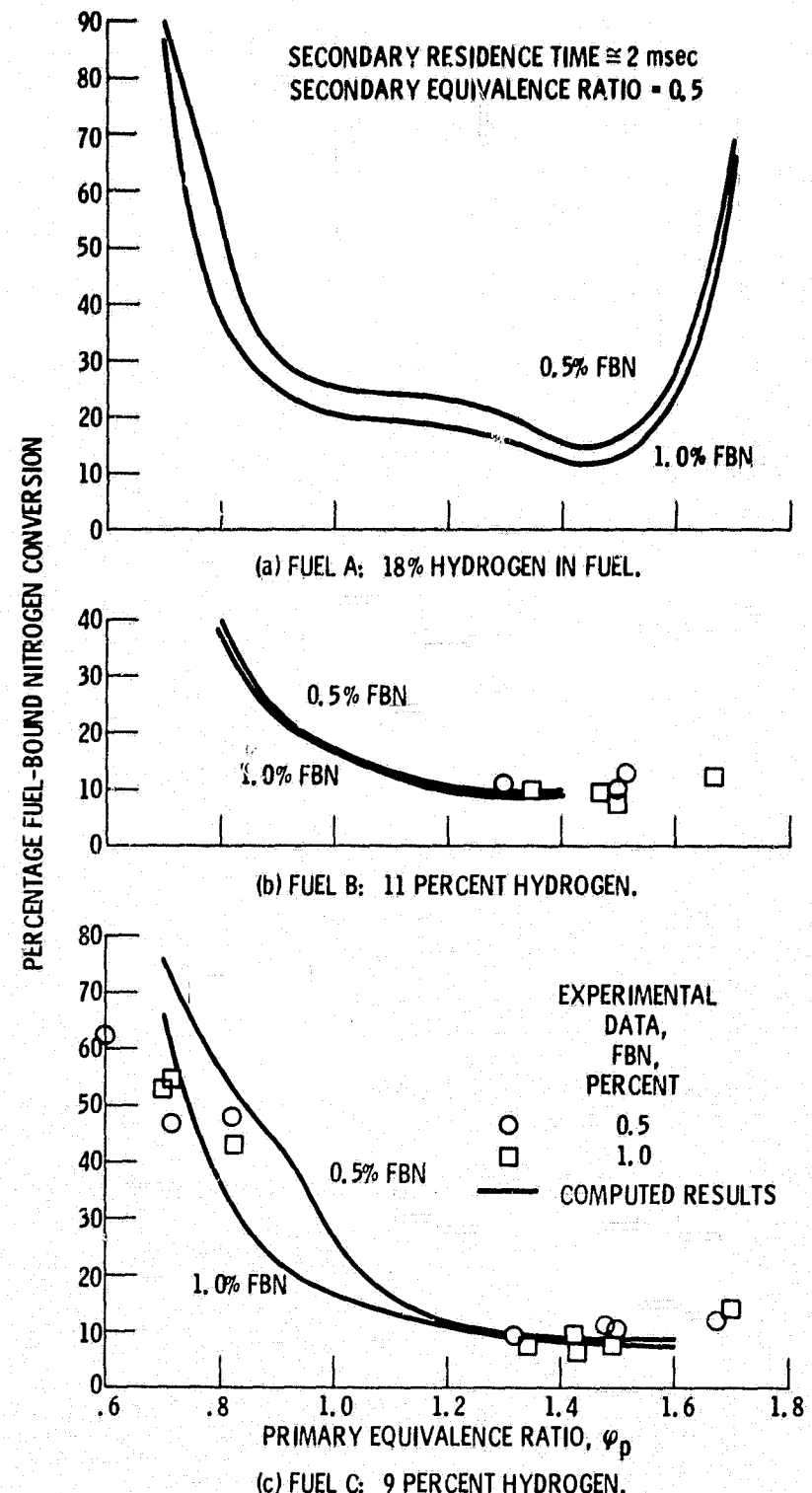

Figure 3. - Fuel-bound nitrogen conversion vs. primary equivalence ratio.

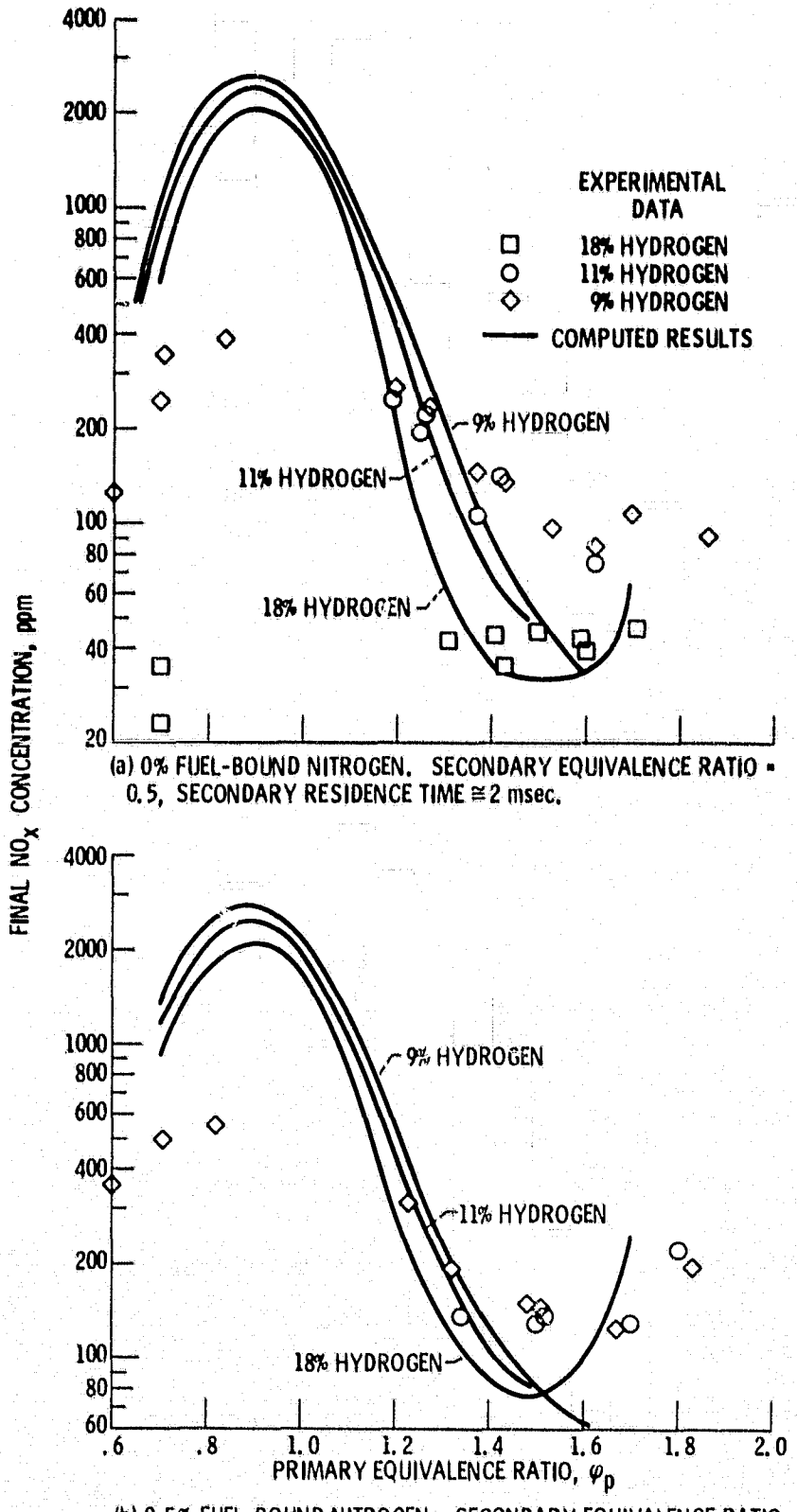

(a) 0% FUEL-BOUND NITROGEN. SECONDARY EQUIVALENCE RATIO = 0.5, SECONDARY RESIDENCE TIME ≅ 2 msec.

(b) 0.5% FUEL-BOUND NITROGEN. SECONDARY EQUIVALENCE RATIO = 0.5, SECONDARY RESIDENCE TIME ≅ 2 msec.

Figure 4. - Effect of hydrogen content on NO_x emissions.

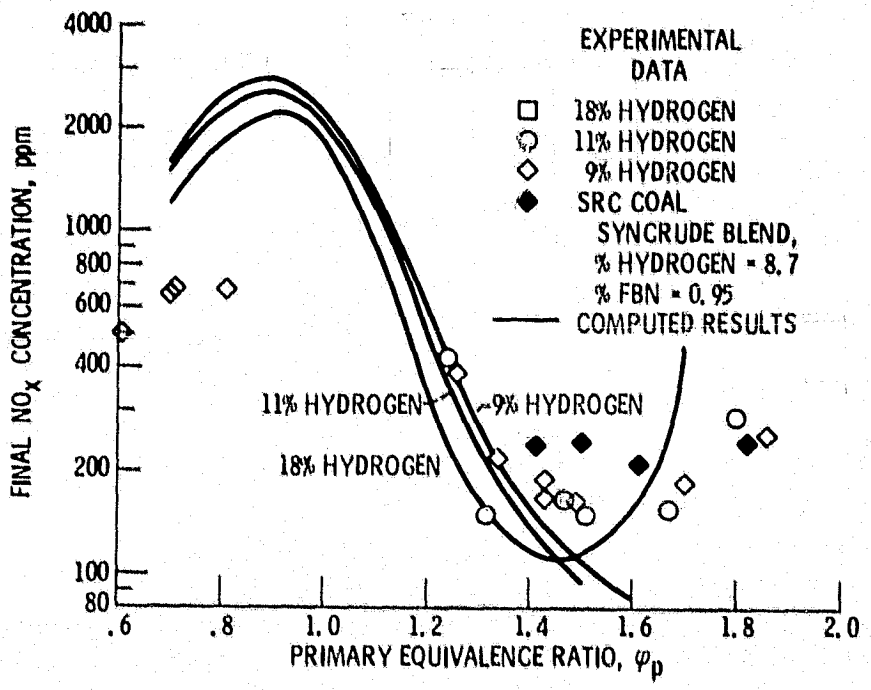

(c) 1.0% FUEL-BOUND NITROGEN. SECONDARY EQUIVALENCE RATIO = 0.5, SECONDARY RESIDENCE TIME ≅ 2 msec.

Figure 4. - Concluded.

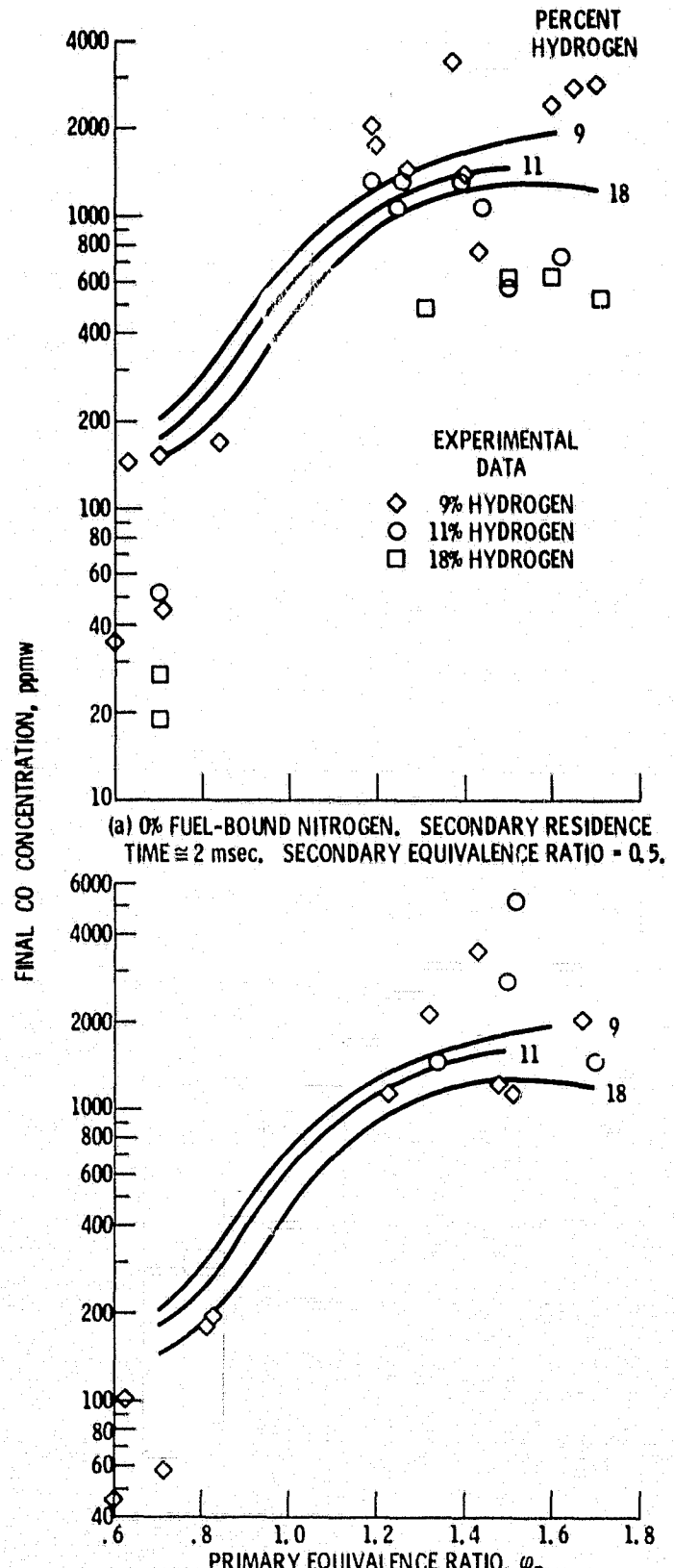

(a) 0% FUEL-BOUND NITROGEN. SECONDARY RESIDENCE TIME ≅ 2 msec. SECONDARY EQUIVALENCE RATIO = 0.5.

(b) 0.5% FUEL-BOUND NITROGEN. SECONDARY RESIDENCE TIME ≅ 2 msec. SECONDARY EQUIVALENCE RATIO = 0.5.

Figure 5. - Effect of percent hydrogen on carbon monoxide emissions for hydrocarbon combustion.

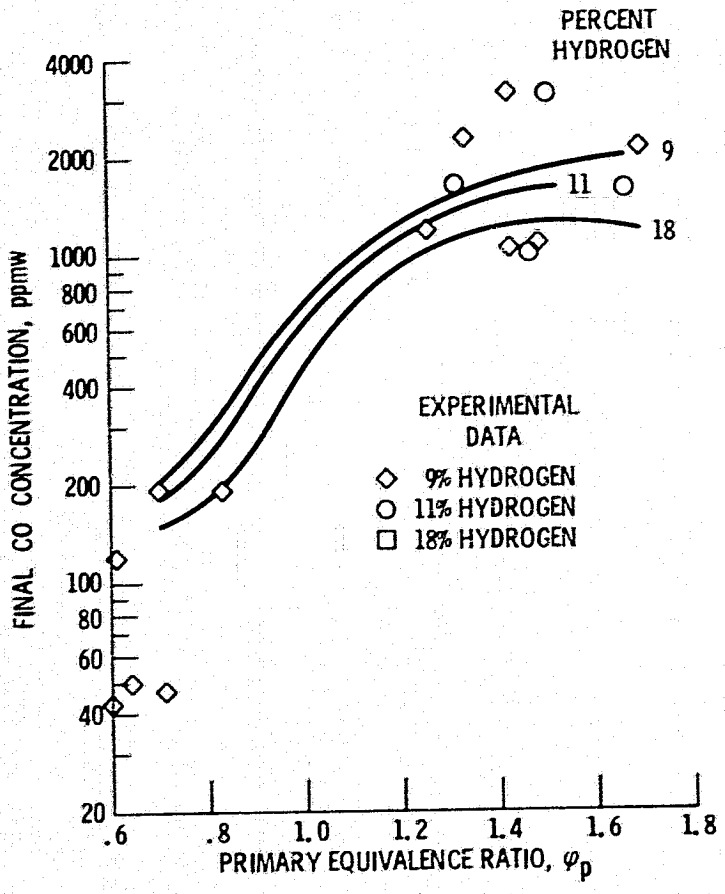

(c) 1.0% FUEL-BOUND NITROGEN. SECONDARY RESIDENCE TIME ≅ 2 msec. SECONDARY EQUIVALENCE RATIO = 0.5.

Figure 5. - Concluded.

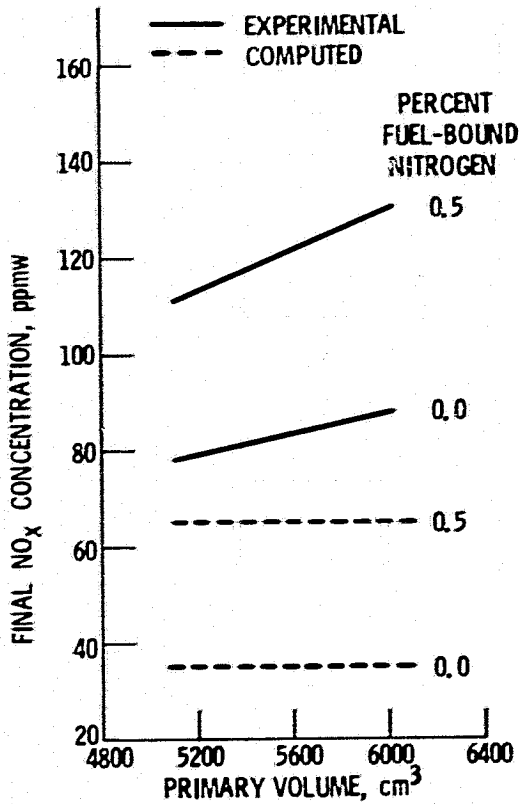

Figure 6. - NO_x concentration vs. primary volume. Fuel C: 9 percent hydrogen; primary equivalence ratio = 1.6, secondary residence time ≅ 2 msec, secondary equivalence ratio = 0.5.

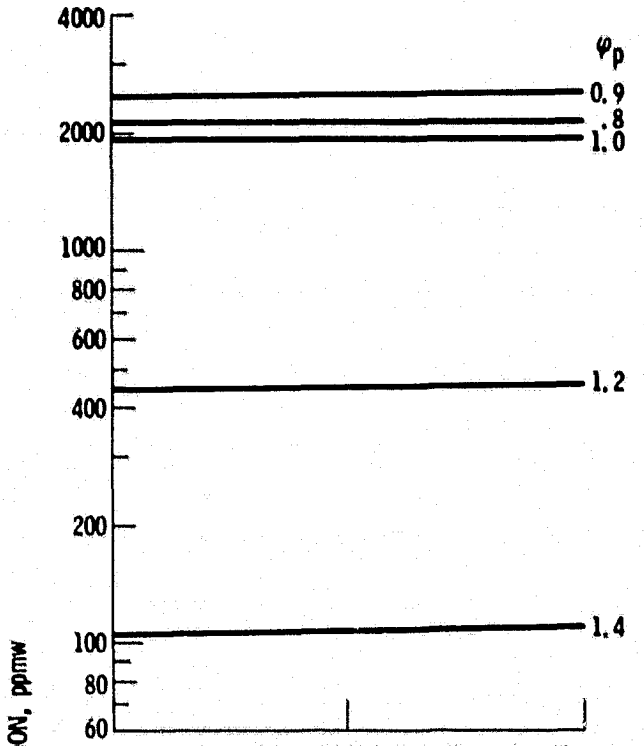

(a) FUEL B: 11 PERCENT HYDROGEN; 0.5 PERCENT FUEL-BOUND NITROGEN.

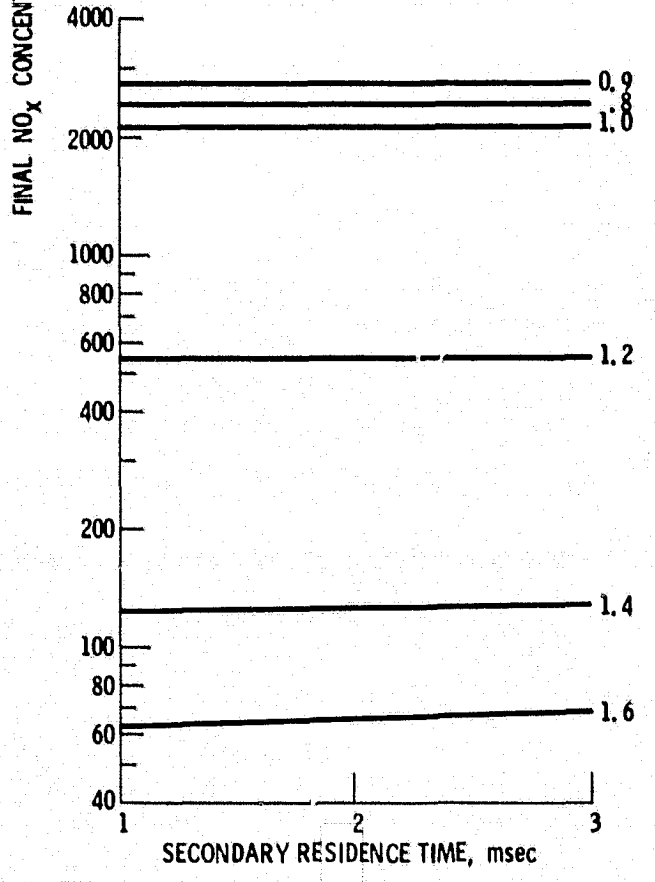

(b) FUEL C: 9 PERCENT HYDROGEN; 0.5 PERCENT FUEL-BOUND NITROGEN.

Figure 7. - Effect of secondary residence time on NO_x formation. Secondary equivalence ratio = 0.5.

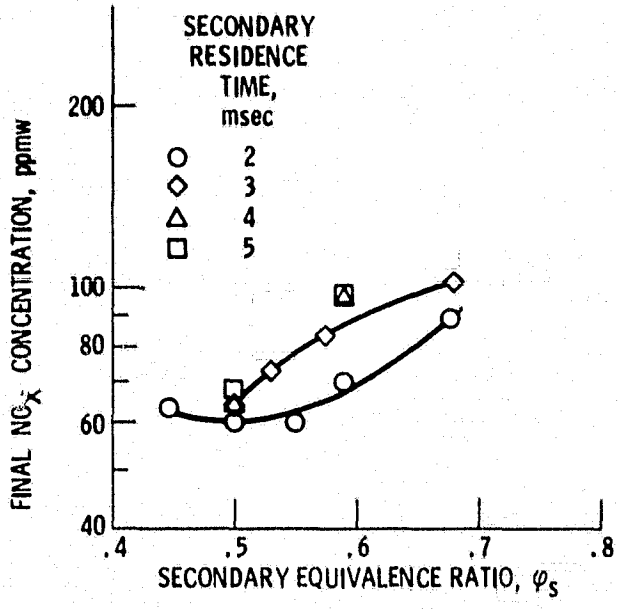

Figure 8. - Experimental final NO_x concentration vs. secondary equivalence ratio for various secondary residence times. Fuel B: 11 percent hydrogen; primary equivalence ratio = 1.5; 0.0 percent fuel-bound nitrogen.

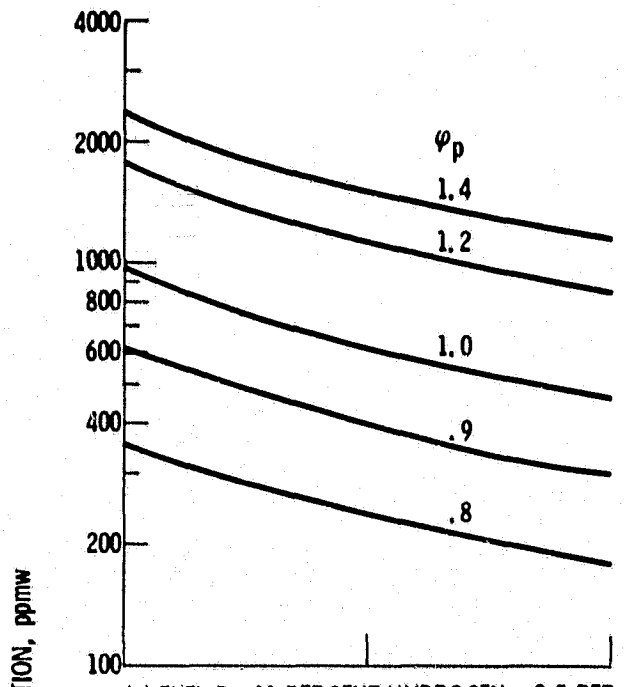

(a) FUEL B: 11 PERCENT HYDROGEN. 0.5 PERCENT FUEL-BOUND NITROGEN.

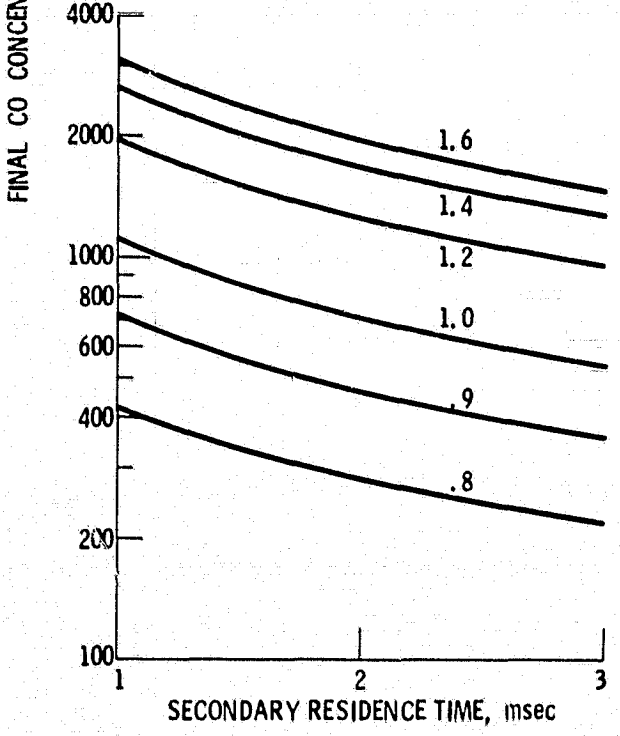

FINAL CO CONCENTRATION, ppmw

(b) FUEL C: 9 PERCENT HYDROGEN. 0.5 PERCENT FUEL-BOUND NITROGEN.

Figure 9. - Effect of secondary residence time on CO formation. Secondary equivalence ratio = 0.5.

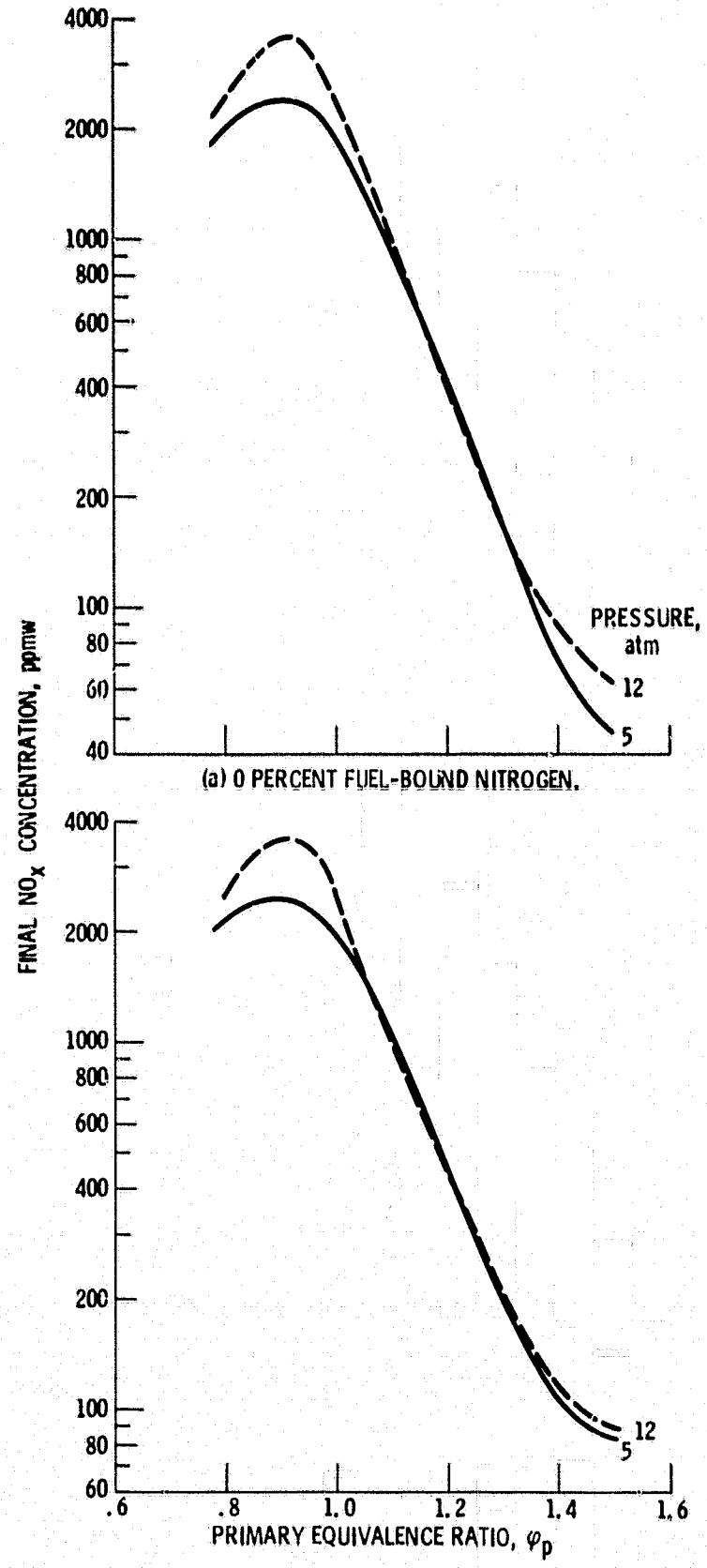

Figure 10. - Effect of pressure on NO_x formation. Fuel B: 11 percent hydrogen; residence time ≅ 2 msec. Secondary equivalence ratio = 0.5.

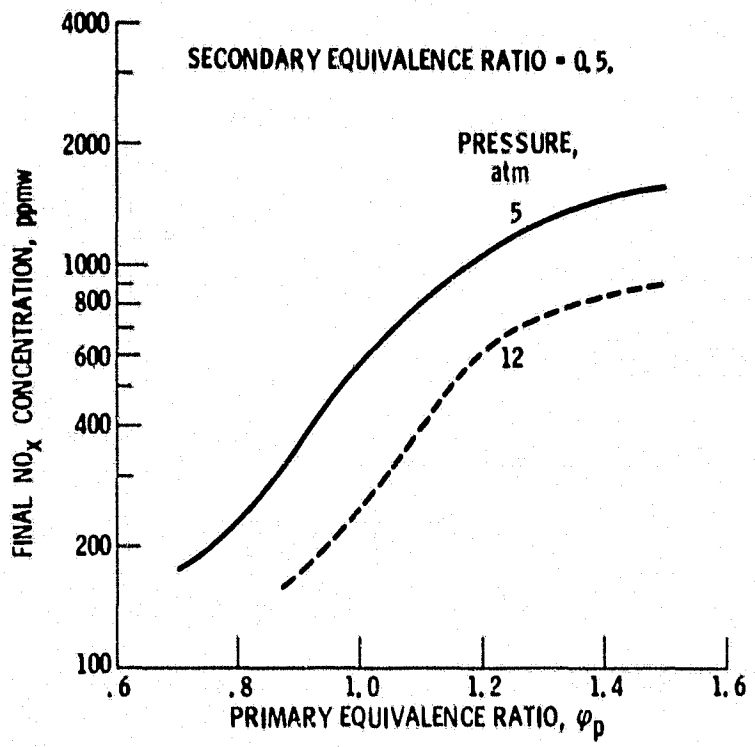

Figure 11. - Effect of pressure on carbon monoxide formation. Fuel B; 11 percent hydrogen; residence time ≅ 2 msec; 0.0 percent fuel-bound nitrogen.